UNIVERSITÉ DE GENÈVE

Analysis, Validation and Radial Velocity Follow-Ups of Exoplanet Candidates from GAIA DR-3

Author:

Avidaan SRIVASTAVA

Department of Astronomy, Observatoire Astronomique de l'Université de Genève

Supervisors:

Prof. François BOUCHY, Angelica PSARIDI

Master Thesis for Astrophysics Lab 1

Date: 23 December, 2022

Analysis, Validation and Radial Velocity Follow-Ups of Exoplanet Candidates from GAIA DR-3

Author:
Avidaan SRIVASTAVA (Department of Astronomy, Observatoire Astronomique de l'Université de Genève)

Supervisors:
Prof. François BOUCHY, Angelica PSARIDI

Abstract

Since its launch in 2013, European Space Agency's (ESA) successor to Hipparcos, GAIA, has done a remarkable job at 3-D mapping the sky. Additionally, it has collected data from over 2 billion objects in the form of photometry, spectrometry and even astrometry. Throughout the years there have been four sets of data release, the latest one being the Data Release 3 (DR3) in 2022. This project aims to look at the Exoplanet Candidates of this data set and perform ground based Radial Velocity follow up using the 1.2-m Swiss Euler Telescope equipped with the CORALIE spectrograph. Moreover, lightcurves from NASA's Transiting Exoplanet Survey Satellite (TESS), for the candidates for those they are available, are used to perform further analysis and obtain various parameters about the candidates such as the radius and period and make comparisons to the values listed in the GAIA Archive.

Contents

Chapter 1

Introduction

1.1 Radial Velocity Method

The very first plant to ever be discovered orbiting a star other than the sun, 51 Pegasi b [1] was detected using the Radial Velocity wobble of the star. Figure 1.1 shows the working of this method of planet detection. If a star has a companion, the physics states that they would both orbit their common center of mass. The position of this center of mass may depend on the separation between the two objects and their masses. For reference, Jupiter being the most massive object orbiting the Sun governs the Solar System's relative center of mass (also know as the Barycenter) which is located just outside the Sun's surface. Equation 1.1.1 gives the relation to calculate the minimum mass of the planet companion ($M_p\, sin\,(i)$) using the measure velocity semi-amplitude (K). When a Radial Velocity Spectrometer (RVS) instrument takes data from a star, it compares the spectral lines and their wavelengths to the standard wavelengths where these lines should appear. If the star has a radial velocity component along our line of sight, due to the Doppler Effect, lines may be Redshifted (moving away) or Blueshifted (moving towards) as shown in Figure 1.

$$K = \left(\frac{2\pi G}{P}\right)^{1/3} \frac{M_p \sin i}{\left(M_\star + M_p\right)^{2/3}} \frac{1}{\left(1-e^2\right)^{1/2}} a_p \tag{1.1.1}$$

The RVS instrument aboard GAIA has collected data from stars throughout the years using this method and has listed 9 potential exoplanet candidates in Data Release 3 (DR3).

1.2 Transit Method

Another technique of detecting stellar companions is the Transit Method. Figure 1.2 gives a graphical demonstration of how this method works. The flux coming from a distant star is measured at short intervals over a long period of time (months to years). This Flux versus time graph is called a lightcurve. When a large enough object passes between us and the star in our line of sight, there is a dip in the flux (brightness) that can be observed. From this (transit depth), a mathematical relation, shown in Equation 1.2.1 can be derived that relates the radii of the star and the companion. The shape of the trough during the transit can also give some valuable information about

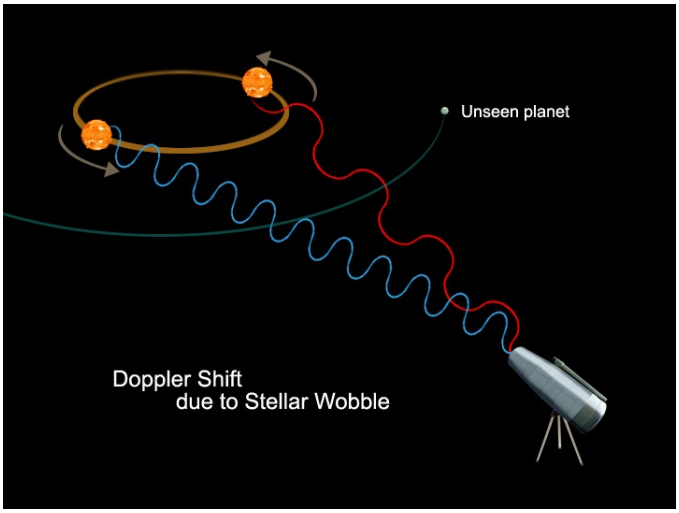

Figure 1.1: Concept behind Radial Velocity exoplanet detection (NASA) [21]

the companion. For example, if it is more V-shaped, there is a high likelihood of it being a star however, if it is U-shaped, then it is likely a planet. GAIA DR3 contains a total of 39 TROIs.

1.2.1 Transiting Exoplanet Survey Satellite (TESS)

If the target star is observed for long enough, multiple transits can be detected and a periodogram can be used to get an estimate of the frequency at which they happen and thereby get the orbital period of the star-companion system. Unfortunately, at the time of writing this, GAIA has not made its lightcurves public, therefore we had to resort to using lightcurves taken by NASA's Transiting Exoplanet Survey Satellite (TESS). TESS was launched in 2018 with the sole objective of detecting transiting exoplanets. TESS was designed to be a high precision photometer and not a imager [22] which is why minimization of background noise took precedence over having a small Point Spread Function (PSF). Since the GAIA candidates were not the high priority TESS candidates, only a fraction of stars had low cadence (flux observed every 30 minutes) lightcurves available.

$$f = \left(\frac{R_{companion}}{R_{star}} \right)^2 \tag{1.2.1}$$

1.3 GAIA

GAIA was launched in 2013 by the European Space Agency with the objective of 3D mapping the entire sky. In its initial mission, GAIA was meant to collect astrometric, photometric and spectrometric data for over a billion stars in the Milky Way and the Local Group by 2019. Since then, it has outlived its initial lifetime and is set to continue up to 2025 and has successfully observed two billion objects.

Currently at the Earth-Sun L2 (Second Lagrange) point, GAIA is equipped with a dual telescope design, each of which are based on the three-mirror anastigmat (TMA) design with a wide focal

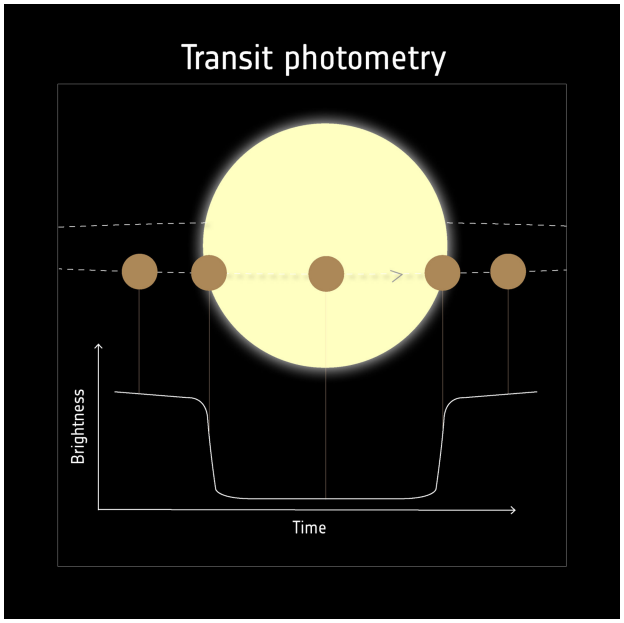

Figure 1.2: Concept behind Transiting exoplanet detection (ESA) [20]

plane [9]. This wide focal plane houses a Charge Coupled Device (CCD) mosaic of 106 CCDs allowing for extremely detailed measurements using almost a billion pixels. The telescope setup allows for a large enough field of view and precision to obtain accurate astrometric data for even the crowded regions of the sky with millions of stars per degree squared.

GAIA's recorded photometric data is taken using the onboard instrument that consists of two dispersers, the Blu Photometer (BP) and Red Photometer (RP) which cover a combined wavelength range from 330-nm to 1050-nm. The spectral density gathered via this instrument gives insight into the stars' temperatures, reddening and even metallicity. The Radial Velocity Spectrometer (RVS) is another critical instrument that records high resolution radial velocity measurements of target stars corresponding to the wavelength range of 845-nm to 872-nm in the near infrared. With the combination of these two instruments, GAIA is capable to detecting possible planetary companions around target stars which are then listed in the subsequent data releases [9].

Since its launch, GAIA has publicly released the collected data through: Data Release 1 (2016) [8], Data Release 2 (2018) [10], Early Data Release 3 (2021) [16] and Data Release 3 (2022) [18]. For this project, we are looking specifically at the exoplanet candidates listed inside the DR3 catalogue. The candidates in DR3 are listed corresponding to their detection method with 39 Transiting Objects of Interest (TROI) (excluding the two already confirmed ones), 9 Radial Velocity Objects of Interest (RVOI) and 73 Astrometric Objects of Interest (ASOI). Some preliminary testing done by Damien Ségransan lead to the conclusion that the ASOIs were mostly false positives, hence why we are only interested in conduction analysis for the TROIs and RVOIs.

1.4 CORALIE

The main objective of this project is to verify if the list of exoplanet candidates in DR3 are actually planets, stars or false positives. To do this, we take Radial Velocity measurements from the ground to follow up on these target candidates. To do this we are using the 1.2-m Euler Swiss Telescope located at the ESO La Silla Observatory in Chile. Th Euler telescope is equipped with the high precision CORALIE Spectrograph that the Observatory of Geneva was involved in building. CORALIE has a resolution of 60,000 [4] and has been operational since 1998. Since then several technical operations have been performed to improve the instrument's optical efficiency and measurement precision (now up to 3-m/s).

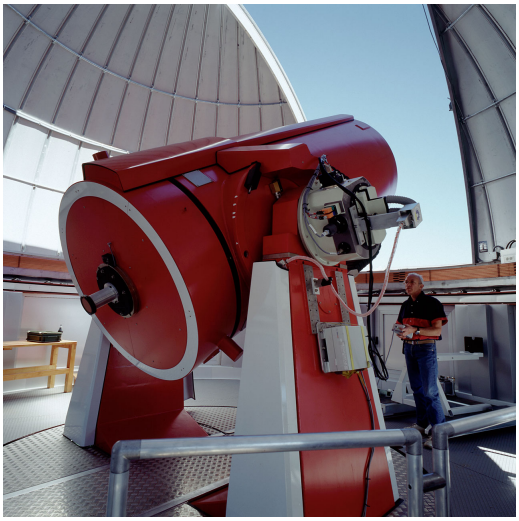

Figure 1.3: 1.2-m Swiss Euler Telescope that houses the CORALIE spectrograph (ESO) [3]

Chapter 2

Target Selection and Analysis

2.1 Target Selection Criteria

Since the list of exoplanet candidates in DR3 was quite extensive (39 TROIs and 9 RVOIs), we created a few selection criteria to filter out the targets we can realistically observe and follow. The criteria depend on the target's visibility from the La Silla site, sensitivity of CORALIE and results from any previous survey that may have observed them.

2.1.1 Visibility

Our only way to make RV follow-up detections is through the Euler Swiss telescope located in Chile, therefore, we can only choose to follow targets that are going to be visible from the southern hemisphere. The duration of this project is from September 2022 to March 2023 which puts another constraint on the visibility of target stars. To keep track of our selected targets, We used the STARALT [5] software that gives an estimate of the position of the target across the sky for a given date, provided the coordinates of said target are known. STARALT also gives a value for the airmass at the time of observation. Looking at the apparent magnitude values of the stars (Figure 2.1) most of the TROIs were fainter than the RVOIs, which can be explained through an observational bias. For CORALIE to actually make the detection, we opted to only observe when the airmass was less than 1.5. However, because of the higher brightness of RVOIs, we had a little more leeway in terms of observation so for these specific targets we chose to make observations even at an airmass of 2. Having an airmass too high can skew our observations by quite a lot so it was an important detail to keep in mind which making the list of eligible targets. After getting all this information, we created a colour coded visibility chart for all the targets so that it becomes easier to allocate telescope time depending on when certain targets will become visible.

2.1.2 CORALIE Sensitivity

As mentioned before, there is a wide range of brightness amongst all the DR3 candidates. The CORALIE spectrograph has a detection limit to give accurate results, therefore we discarded all the targets that seemed to have a V-mag value of more than 13.5. Another key note, to optimize telescope time, a limit on the exposure time was set depending on the brightness of the target. The

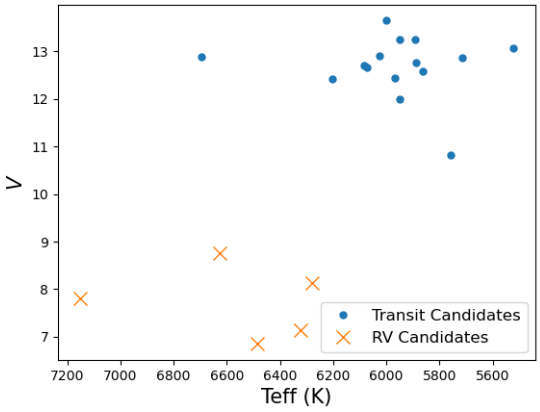

Figure 2.1: Graph displaying the V-mag versus T_{eff} of the final 20 candidates selected separated according to their detection method

RVOIs were much brighter than the TROIs so the exposure time for them was lower. Finally we settled on 1800 seconds for TROIs and 900 seconds for RVOIs.

2.1.3 Other Survey Results

Throughout the years there have been several sky surveys that have likely observed the same part of the sky where GAIA found the exoplanet candidates. If data for the DR3 targets has been analyzed and a conclusion has been reached, it makes sense to discard those candidates as well. Two of our candidates, GAIA-TROI-020 [12] and GAIA-TROI-022 [12] were confirmed to be part of a binary system and not a planetary candidate.

Once all of these criteria were set, we filtered out all the candidates from DR3 that failed to meet one or more of these criteria. In the end a total of 15 TROIs (B.3) and 5 RVOIs (B.5) remained that we can follow and attempt to come to a conclusion about.

2.2 Analysis

Before making observations via CORALIE, or between observations, there is some important information about the planetary candidates and their stars that we need to finalize such as the radii of the star and the planet, effective temperature of the star, and period of the star-companion system. The best place to get, or derive, these parameters is through the GAIA Archive which lists all the available information GAIA has collected about said candidate, identified using the GAIA ID, over the years.

For both the TROIs and RVOIs, GAIA Archive had the effective temperature of the star (T_{eff}), G-band mean magnitude ($G - mag$), Integrated BP and RP mean magnitudes (G_{bp} and G_{rp}), distance to the star (in parsecs), the right ascension (RA) and declination (DEC). From all this data several other parameters of the star can be derived using mathematical relations. Since we used V-mag to include or discard candidates for our follow-up, we first calculated V-mag from

$G-mag$, G_{bp} and G_{rp} given by Equation 2.2.1 [17]. The V-mag, along with the distance, can then be used to find the absolute magnitude of the star (M_v) using Equation 2.2.2, where d_{pc} is the distance to star in parsecs.

$$V = G + 0.02704 - 0.01424\,(G_{bp} - G_{rp}) + 0.2156\,((G_{bp} - G_{rp}))^2 - 0.01426\,(G_{bp} - G_{rp})^3 \quad (2.2.1)$$

$$M_v = V - 5\,(log\,(d_{pc}) - 1) \quad (2.2.2)$$

Since this M_v is a measure of the luminosity of the star relative to the solar luminosity (Equation 2.2.3) and then finally a Mass-Luminosity relation can be used to get an estimate of the stellar mass as shown in Equation 2.2.4 [15]. It should be noted that the Mass-Luminosity relation used here is only valid for stellar masses or greater than $0.7M_\odot$ which can be justified for use based on Figure 2.1 showing the effective temperatures corresponding to majorly F-type stars which makes them approximately equal to or more massive than the sun. Additionally, with the Luminosity and T_{eff} values, an estimate of the stellar radius (R_*) can be obtained from Equation 2.2.5, where σ is the Stefan-Boltzmann constant.

$$\frac{L_*}{L_\odot} = 100^{(4.83-M_v)/5} \quad (2.2.3)$$

$$\frac{M_*}{M_\odot} = \frac{1}{1.02} \times \left(\frac{L_*}{L_\odot}\right)^{(1/3.92)} \quad (2.2.4)$$

$$L_* = 4\pi R_*^2\,\sigma\,T_{eff}^4 \quad (2.2.5)$$

2.2.1 TESS Lightcurves

As mentioned previously, NASA's TESS has been observing the whole sky, looking for transiting exoplanets and throughout that process it has also observed some of the targets passively. None of the DR3 candidates have a TESS Input Catalogue identifier (TIC) except for GAIA-TROI-012 so we cannot use the TESS pipeline and *lightkurve* [11] to extract the lightcurves. However, thanks to our collaborators at Tel Aviv University, we were able to obtain the TESS lightcurves for some of the TROIs (11 out of the selected 15).

Because TESS only observed these targets in the background, it only took a snapshot of the stellar flux every 30 minutes (low cadence) instead of the high cadence (2 minutes) reserved for TIC targets. These low cadence lightcurves had the drawback of not giving very accurate values for the transit depth or the period however if multiple transits were observed, the phase folded lightcurve could help mitigate that issue to an extent. Once the normalized lightcurve was obtained we used GAIA's ephermeris (Period and Epoch time), which were available on the GAIA Archive for the TROIs, as an estimate and ran a Box Least Squares (BLS) periodogram to get the actual period of the system. BLS and Lomb-Scargle (LS) are the two major periodograms used in transit photometry. BLS is better used to get an estimate of the frequency at which the transits happen whereas LS periodogram helps in getting information about the variability of the star's brightness. Figure 2.2 shows the lightcurve, BLS and LS periodograms of one of our targets, GAIA-TROI-012 as an example. The low cadence lightcurve is clearly identified here.

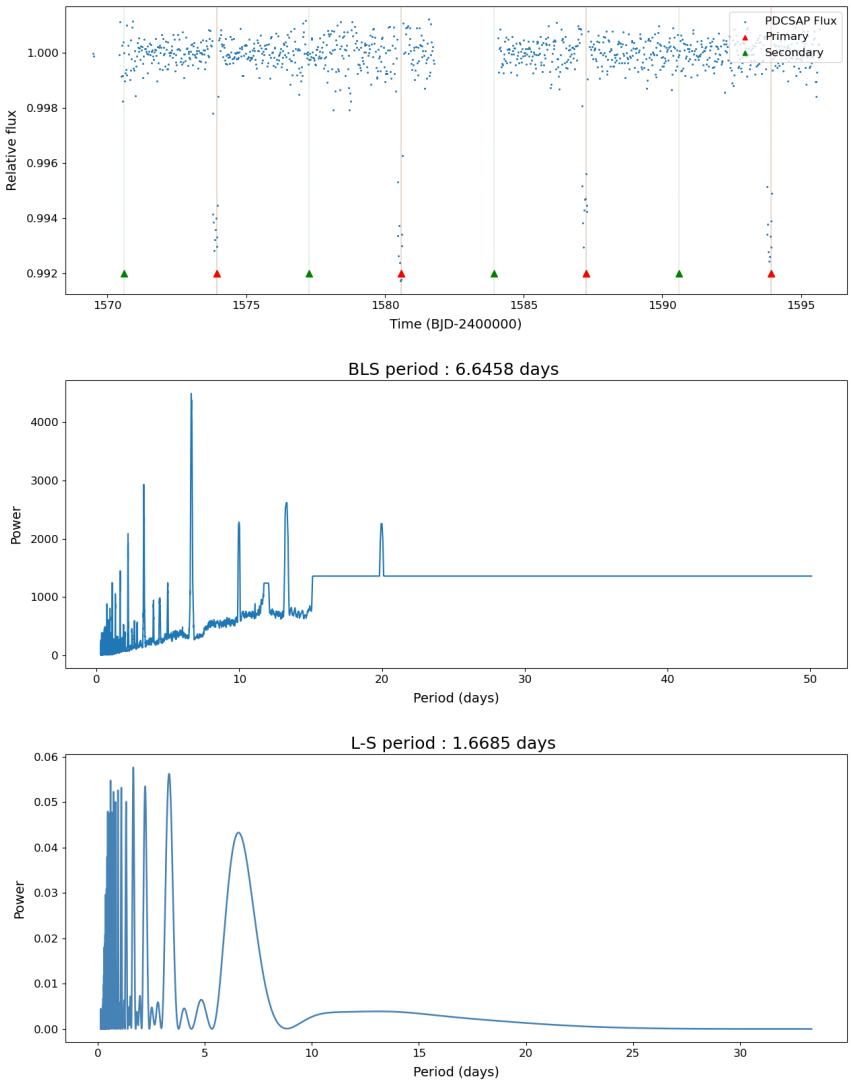

Figure 2.2: Normalized Lightcurve, BLS Periodogram, LS Periodogram of GAIA-TROI-012

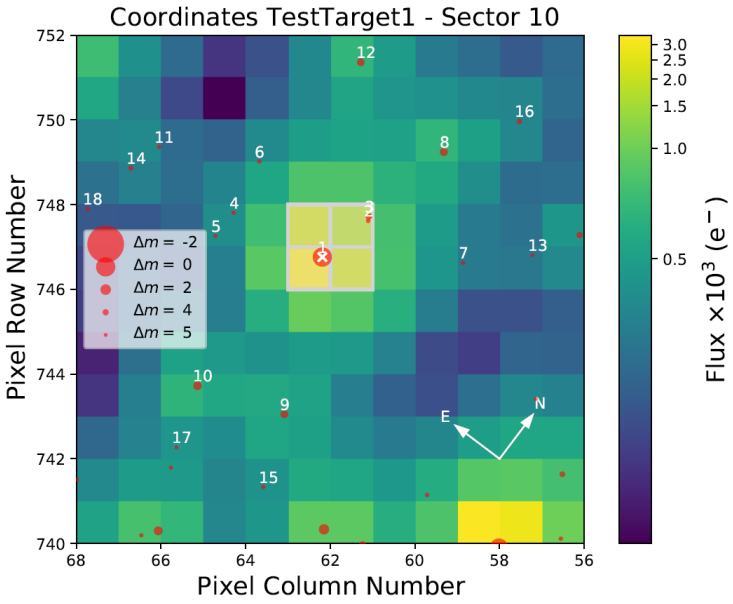

Figure 2.3: TPF of GAIA-TROI-012

Additionally, the Data and Analysis Center for Exoplanets (DACE) platform, a part of the astronomy department at University of Geneva, has the *BATMAN* [7] program available to use which for a given lightcurve does some further computing, including running an MCMC sampler, to get more accurate measurements of the transit depth, ratio of the star and companion radii and epoch times. After inputting the stellar radii we derived previously, we computed the radii of the companions as well, corresponding to the transit depth observed by TESS. It is of note that the GAIA Archive also provided transit depths for TROIs so comparisons can be made for both the period and transit depth acquired by TESS and GAIA.

To get a better idea of how the TESS lightcurves were created, we even extracted the Target Pixel Files (TPF) that TESS had recorded using the *tpfplotter* [14] [1] program available on Github. Unfortunately it was only able to give us the TPFs of 5 TROIs and 3 RVOIs. To make up for this, we used the *Aladin* [2] sky atlas to check for any nearby contaminants for the targets. Figure 2.3 shows an example of a TPF for one of our targets. The 'x' marker in the center is our target star and the white box around it marks the pixels from which the flux was extracted to create the lightcurve. The TPF is immensely helpful in analyzing the contamination effects from the flux from any close, neighbouring stars that may have affected the target's lightcurve.

2.2.2 CORALIE Follow-Up

The DACE platform [13] hosted by UNIGE is the primary way we access our RV data collected by CORALIE. It also has an inbuilt function to model radial velocity curves using the datapoints collected for given set of parameters. The parameters needed to fit a RV curve are: Period, Semi-

[1] This work made use of `tpfplotter` by J. Lillo-Box (publicly available in www.github.com/jlillo/tpfplotter), which also made use of the python packages `astropy`, `lightkurve`, `matplotlib` and `numpy`

Amplitude, Eccentricity and Epoch time. There are options to fill in the period using an inbuilt periodogram provided there are enough datapoints collected.

There need to be at least three datapoints for a given target in order to properly fit an RV curve and use its results. For most of the candidates, for which we have enough datapoints, we tested both the GAIA and TESS period while fitting the RV curve to see which one was the more accurate one, if there was a discrepancy. There is also a feature to get an estimate of the mass of the companion from the RV fit, provided the mass of the star is known (Equation 1.1.1). AT this point, we cannot get an estimate of the angle of inclination of the star-companion orbit (i) relative to our line of sight. Since we got estimates of mass of the star earlier, we were able to get results for mass of the companions as well.

2.2.3 Spectroscopy Data

When CORALIE records data from a target star, it gives a very important result in the form of the Cross Correlation Function (CCF). A CCF is a mathematical process in which the spectrum of a star is multiplied by a weighted binary 'mask', usually corresponding to the spectral type of the star, and then finding the minimum of the result as a function of the Doppler shift [6]. Since the star has some velocity along our line of sight, the spectral lines are shifted due to the Doppler Effect. Hence, why the CCF is extremely important in getting information about the star's radial velocity at the time of taking the spectrum.

However, that is not the only use of the CCF. The CCF can be seen as an 'average absorption line' and because of that, it should ideally have a single peak, corresponding to a single star. Figure 2.4 (a) is an example of the CCFs of multiple datapoints taken from the same target an overlapped on to each other. The symmetry is to be noted here. Figure 2.4 (b) on the other hand shows another CCF of a different target which is clearly asymmetric. This asymmetry arises due to the presence of another star who's peak is 'blended' in with the peak of our target. This is what is known as a Spectroscopic Binary (SB), which confirms the companion of our target to be a star and not a planet.

Another key property of a CCF is its width. The wider it is, the faster the star's rotation and vice-versa. Because of the asymmetry discussed previously, the Full Width Half Maximum (FWHM) of the CCF can be correlated to the RV values if it is a SB as both the peaks may move at different speeds relative to each other. Similarly, the Bisector (line that divides CCF through its midpoint) can also show a correlation with the RV in case of SB. The FWHM and Bisector variation can be seen directly on the DACE platform and is important to keep track of so as to identify the targets where the CCF asymmetry is not as obviously seen.

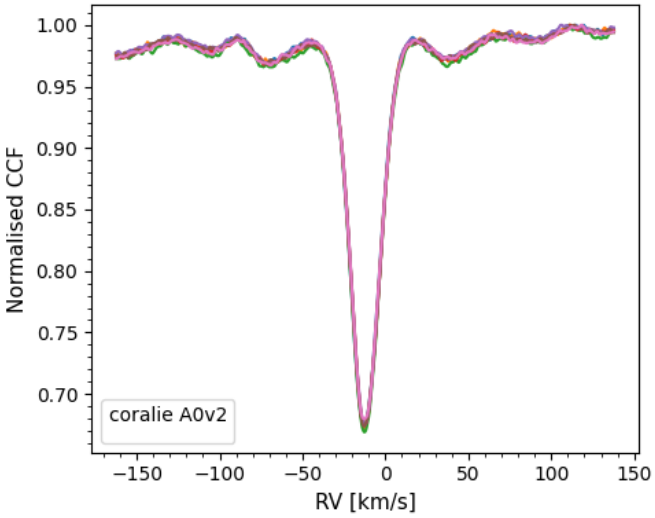

(a) GAIA-RVOI-009

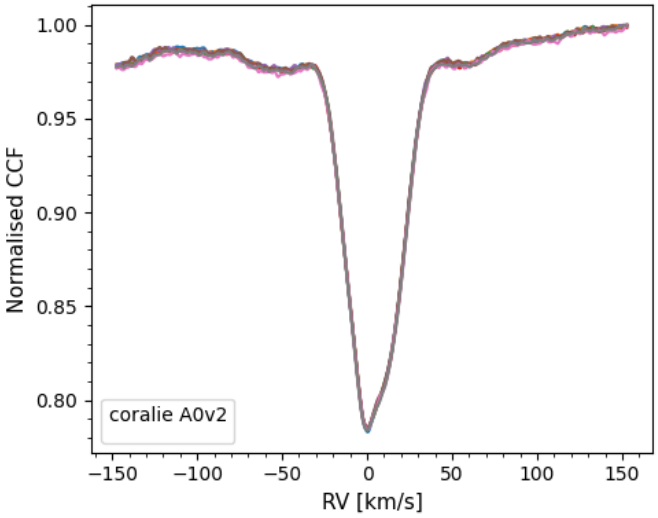

(b) GAIA-RVOI-006

Figure 2.4: Comparing the CCFs of two targets. (a) Symmetric CCF implying the presence of only one star. (b) Asymmetric CCF as a sign of Spectroscopic Binary

Chapter 3

Results

3.1 Overall Results

After completing the analysis for all the 15 TROIs and 5 RVOIs some overall results were obtained that applied to most, if not all, the targets. The major one being the discrepancies between TESS and GAIA's transit depths and period for the TROIs. TESS, as mentioned before, has a much larger PSF (1 arcminute) compared to GAIA which leads to a slightly skewed normalized lightcurve of stars that are in a crowded region because some light from the neighbouring stars gets included in the lightcurve as well. This in turn makes the transit depth smaller than what it should have been, hence explaining why all of GAIA's transit depths are much larger than TESS'.

The periods on the other hand can be explained by GAIA's sampling rate. TESS took the flux data every 30 minutes, however GAIA does it every few days or occasionally twice a day. Because of this, sometimes GAIA doesn't give the actual period of the system but a multiple or a fraction of the period (also called an Alias). This result is better verified and explained for the specific case of GAIA-RVOI-008. For the RVOIs specifically, GAIA's semi-amplitudes (K) were made available by the 'exoplanet.eu' team [19] on their website which we compared to the K values we obtained from RV fits of CORALIE data. The highlight being, none of the GAIA semi-amplitudes match our measured ones.

Over the course of this project, a total of 11 TROIs out of the selected 15 had an available TESS lightcurve, 4 of which did not give a clear indication of a transit occurring because of the high variability of the star's flux seen in the lightcurve. Out of all the TROIs, only 5 had a TPF, and so did 3 out of the 5 RVOIs. 7 of the 20 targets have so far been observed by CORALIE and 2 of them (GAIA-RVOI-008, GAIA-RVOI-006) can be confirmed as spectroscopic binaries, 1 is a false positive (GAIA-RVOI-009), 1 seems to pass all the tests to confirm as an exoplanet (GAIA-TROI-013) while the others do not have enough measured datapoints to come to a definite conclusion. The total observation time amounted to 3 nights and observations were made on 16 different nights. All of the important results are highlighted in the form of several tables listed in Appendix B. Table 3.1 lists out all the targets that have been followed by CORALIE and their respective conclusions we reached by the end of this project.

Table 3.1: Final conclusions about the targets that have been followed by CORALIE

Name	Status
TROI-007	Not SB2
TROI-013	Possible planet
TROI-016	Indeterminate
TROI-017	Indeterminate
RVOI-005	Possible Brown Dwarf
RVOI-006	SB2
RVOI-008	SB2
RVOI-009	No companion

3.2 TROIs

3.2.1 GAIA-TROI-005

TROI-005 was one of the candidates that was observed by TESS at a 30-minute cadence. Figure 3.1 shows the phase folded lightcurve of the target that shows a clear dip signifying there there was a noticeable transit by a planet. The transit depth measured through this TESS lightcurve is 4.021-mmag which corresponds to a planet radius of 0.636 R_J. GAIA however overestimated the transit depth and gave a value of 15.0227-mmag which could be because of TESS' large PSF. However, after comparing the period of the system as observed by TESS and GAIA, the ratio came out to be either 13/9 or 16/11. As the error for GAIA periods is unknown, we cannot given an exact value of this ratio. This target just started to become visible and therefore does not have CORALIE data yet.

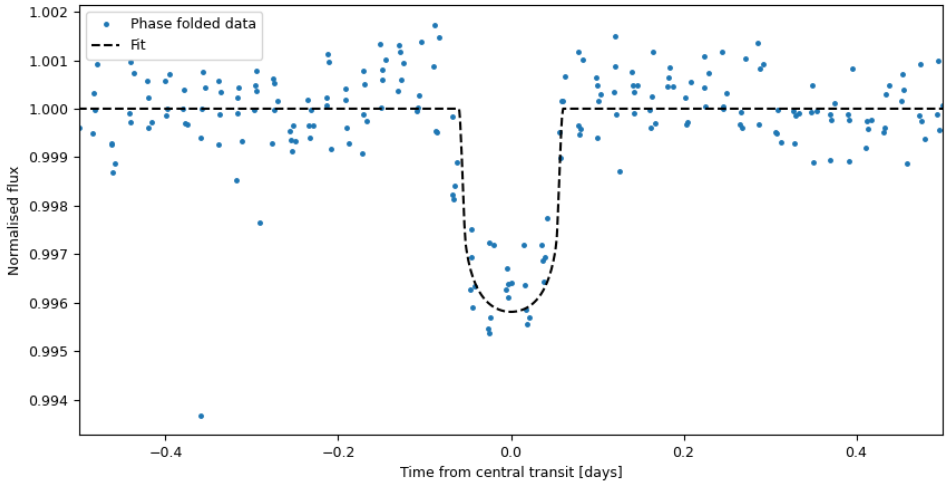

Figure 3.1: Phasefolded TESS lightcurve of GAIA-TROI-005

3.2.2 GAIA-TROI-007

TROI-007 was one of the targets that lacked a TESS lightcurve and so far has not been observed by CORALIE more than once. Taking a look at the CCF (Figure 3.2), there is a slight variation at the peak which is at the order of magnitude of the noise. Otherwise, the CCF is symmetric and the prospect of this candidate being a spectroscopic binary can be ruled out in that regard at the least. The thin CCF also points towards the star being a slow rotator.

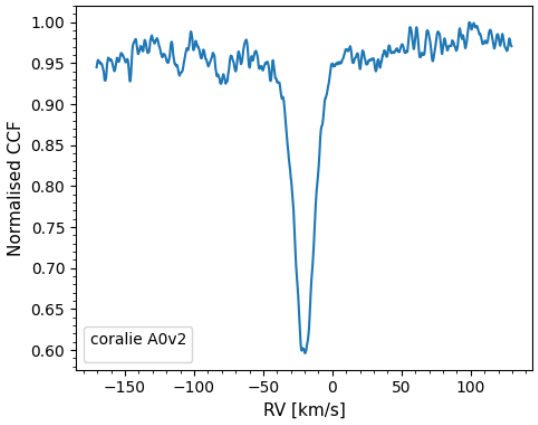

Figure 3.2: CORALIE measured CCF of GAIA-TROI-007

3.2.3 GAIA-TROI-012

TROI-012 indeed had a TESS lightcurve as shown in the phase folded lightcurve (Figure 3.3) which gave a transit depth of 6.459-mmag contrary to GAIA's transit depth of 18.6382-mmag. The planet radius corresponding to TESS transit depth was 1.296 R_J. The periods as measured by TESS and GAIA didn't line up either. The ratio of TESS period to GAIA period was approximately 16/9. This target just started to become visible late December and will be observed by CORALIE in the coming weeks.

3.2.4 GAIA-TROI-013

TROI-13 was one of the few targets that showed very strong signs of being a viable planetary candidate. Both the GAIA and TESS period aligned with a value of 1.53 days. There was also a TESS lightcurve available and CORALIE took several measurements of the target star at various RV phases as shown in Figure 3.4 which represents a fairly regular sine wave passing through the data points consistent with the F0 mask. This RV model corresponds to a planet of mass 1.896 M_J and from the TESS lightcurve (Figure 3.5), the planet radius came out to be 1.02 R_J. Unfortunately GAIA once again overestimated the transit depth. However, the CCF from the CORALIE datapoints seem to be symmetric and there appears to be no FWHM or Bisector correlation hence solidifying this as a strong exoplanet candidate.

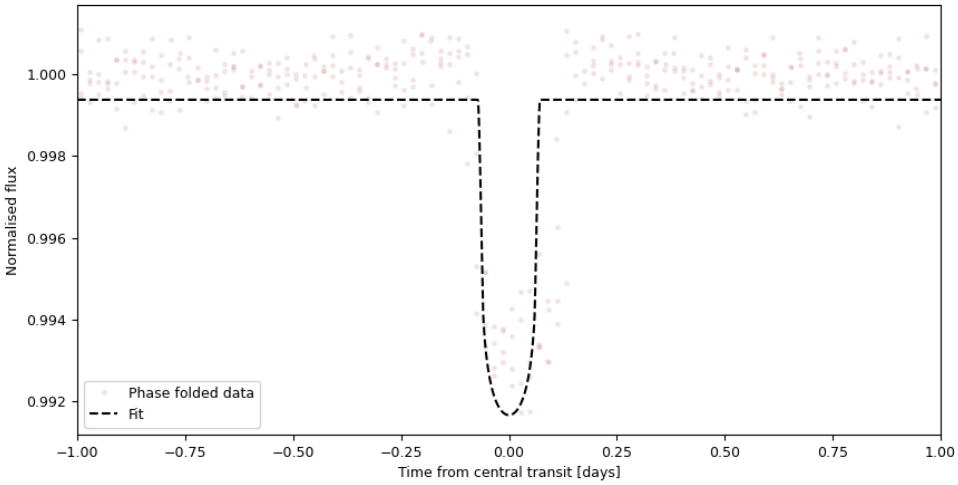

Figure 3.3: Phasefolded TESS lightcurve of GAIA-TROI-012

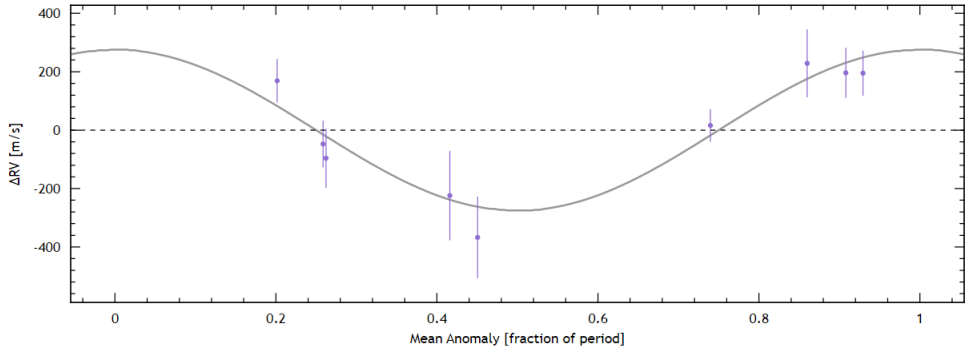

Figure 3.4: RV fit of CORALIE datapoints of GAIA-TROI-013

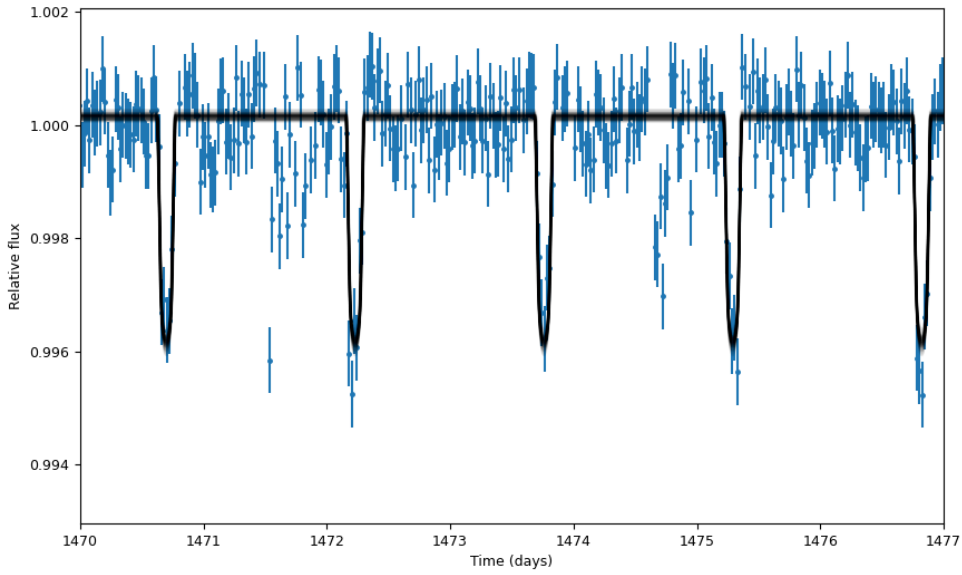

Figure 3.5: TESS lightcurve of GAIA-TROI-013

3.2.5 GAIA-TROI-014

TROI-014 will be visible starting February therefore it has not yet been observed by CORALIE. However, we do have the TESS lightcurve for this target which measured the same period as that measured by GAIA. Additionally, the planetary radius was found to be 1.482 R_J.

3.2.6 GAIA-TROI-016

Similar to TROI-007, TROI-016 lacked a TESS lightcurve and only one datapoint was observed for this target so far, for which the CCF is displayed in Figure 3.6. The variation in the peak looks to be at the order of magnitude of noise, outside of which the curve looks to be symmetrical, ruling out a spectroscopic binary.

3.2.7 GAIA-TROI-017

TROI-017 had both the TESS lightcurve and CORALIE observations. TESS and GAIA period were very consistent with a ratio of 3/1. Figure 3.7(a) is the Target Pixel File (TPF) of TROI-017 which shows the extremely bright star right next to the target which makes it difficult for CORALIE to accurately pinpoint and follow it. Because of that issue we got several datapoints for the supposed target but with drastically different CCFs, indicating that the telescope took measurements of the wrong target (Figure 3.7(b)). This delayed our analysis for this target and so far we don't have anything to report.

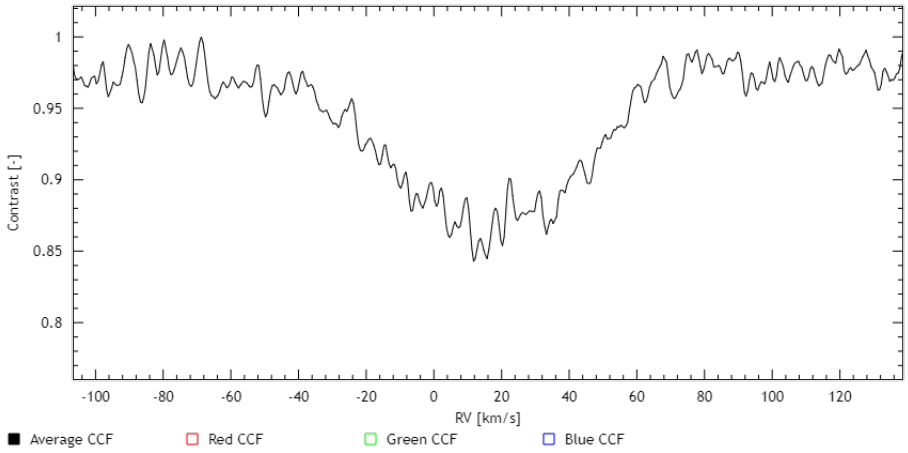

Figure 3.6: CORALIE measured CCF of GAIA-TROI-016

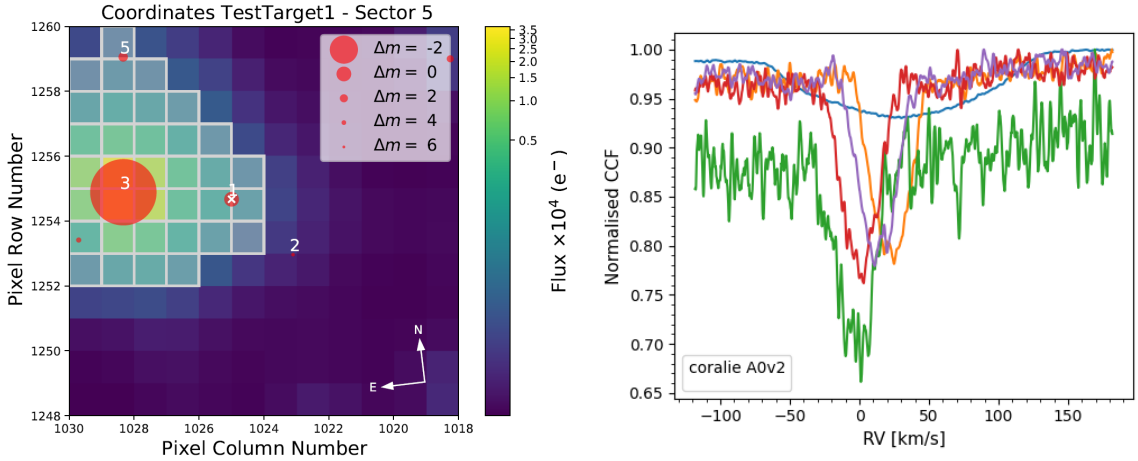

(a) GAIA-TROI-017 TPF

(b) GAIA-TROI-017 CCFs

Figure 3.7: (a) TPF of TROI-017 showing the extremely bright star next to it. (b) Overlapped CCFs of various datapoints of TROI-017 taken by CORALIE. The blue CCF is likely the large bright star as evident from the broad curve (fast rotator). Th green CCF is an unknown target and looks extremely noisy, a possible detection of a faint star. The remaining three CCFs look quite similar which might refer to the actual target.

3.2.8 GAIA-TROI-021

Figure 3.8 contains the phasefolded lightcurve of TROI-021 and there is a clear dip in the lightcurve corresponding to a planet of radius equal to 1.746 R_J. This is also one of those targets where GAIA didn't measure an alias of the period and reported approximately the same period as TESS. TROI-021 will start to become visible in January and hence has no CORALIE data collected yet.

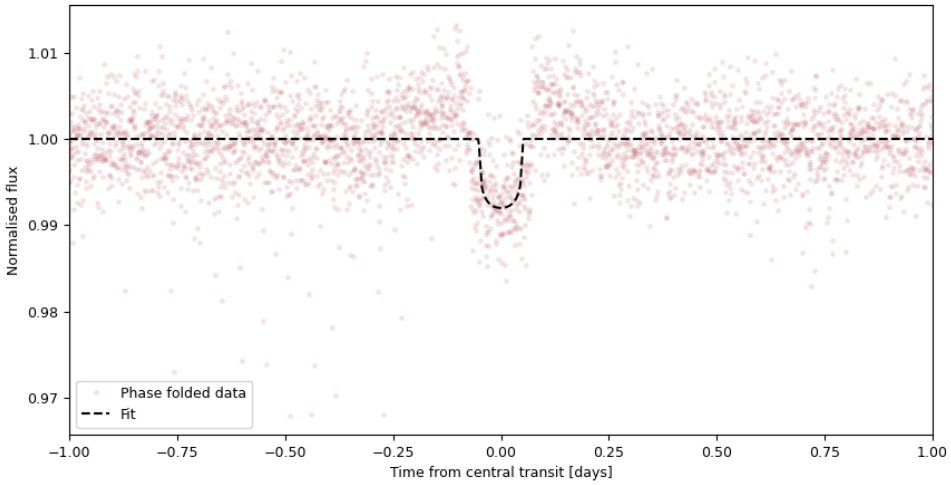

Figure 3.8: Phasefolded TESS lightcurve of GAIA-TROI-021

3.2.9 GAIA-TROI-024

As with TROI-016, TROI-024 doesn't have a TESS lightcurve and has not yet been observed by CORALIE since it will start to become visible by March. Therefore, there is nothing to report for this target.

3.2.10 GAIA-TROI-025

The phasefolded TESS lightcurve for TROI-021 is visualized in Figure 3.9 which gives a planet of radius 0.422 R_J. However, it should be noted that the flux from the star which the candidate orbits is highly variable and it was somewhat challenging to get a clear transit depth from the low cadence TESS measurements which might be further backed by the inconsistent GAIA transit depth which differed by more than 18-mmag. However, the TESS and GAIA periods did in fact give a 3/2 ratio which supports the fact that the transit is real and it's just the depth that might be inaccurate. TROI-25 is additionally quite dim (V-mag = 13.8) which is on CORALIE's limiting side and has therefore not been observed yet in order to divert telescope time to the more important and easier to see targets.

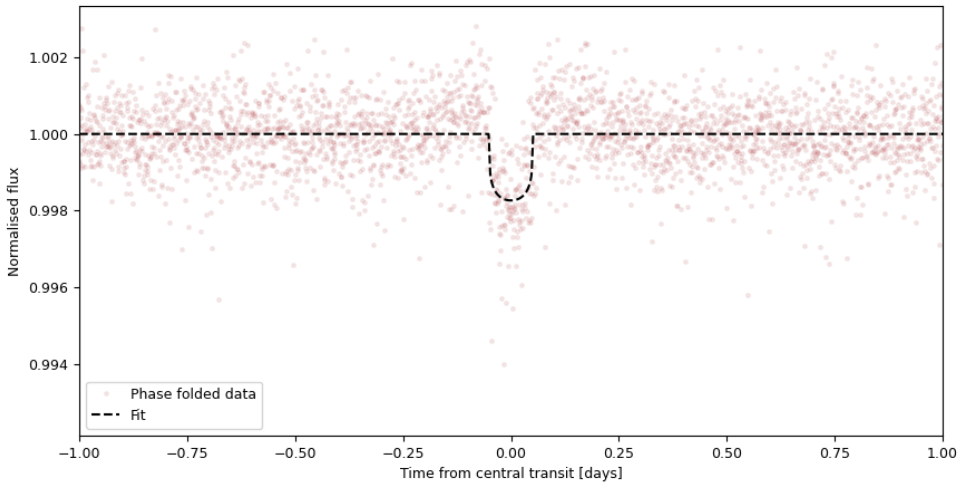

Figure 3.9: Phasefolded TESS lightcurve of GAIA-TROI-025

3.2.11 Other TROIs

TROI-026, TROI-028, TROI-029, TROI-031 and TROI-039 all had TESS lightcurves, with the exception of TROI-039, but the star was too active and gave a fluctuating lightcurve and no clear transit was observed which TESS' low cadence might have contributed to. Since we observed no evidence of there being a planet around these stars, they were not scheduled to be followed up by CORALIE.

3.3 RVOIs

3.3.1 GAIA-RVOI-004

None of the RVOIs had TESS lightcurves despite some of them having a TESS Input Catalogue (TIC) number. RVOI-004 was the only RV candidate to not be followed up by CORALIE because of it being visible in February.

3.3.2 GAIA-RVOI-005

Figure 3.10 shows the RV curve for this target which only consists of three datapoints. Unfortunately, RVOI-005 stopped being visible halfway through the project which made it impossible to get more data. However, it will be visible again in March and will be observed as soon as possible. One datapoint in the RV curve misses the fit and the CCFs of all three points seem to be symmetric with no correlations in the FWHM and Bisector graphs so for now, there are not signs that point towards this target being a Spectroscopic Binary. However, the RV fit corresponds to a very high semi-amplitude, giving a calculated mass of the companion to be 29.37 M_J which could likely be a Brown Dwarf, but we need more data to verify this claim.

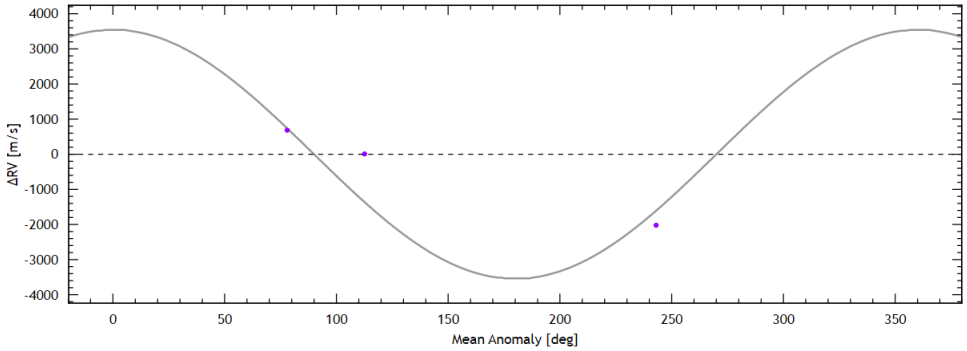

Figure 3.10: RV fit of CORALIE datapoints of GAIA-RVOI-005

3.3.3 GAIA-RVOI-006

The CCF from CORALIE of RVOI-006 is displayed in Figure 3.11 which depicts a clear asymmetry. As mentioned previously in the report, an asymmetric CCF is a clear sign of a Spectroscopic Binary.

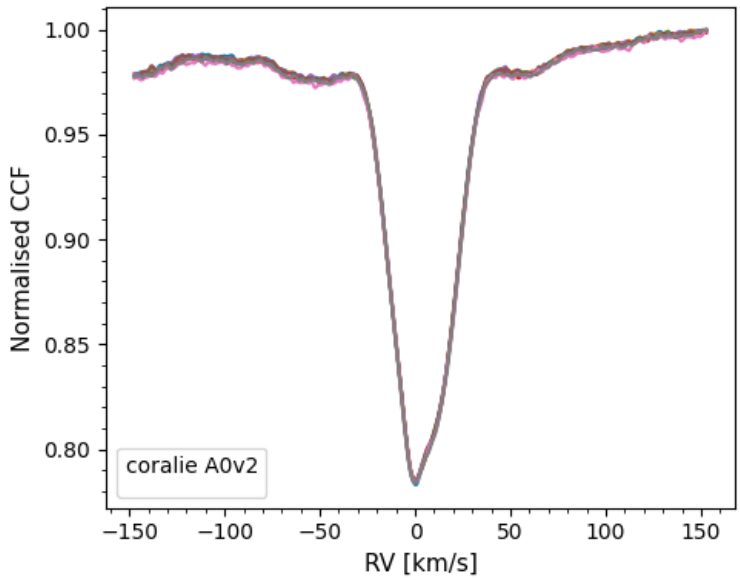

Figure 3.11: Asymmetric CCF of GAIA-RVOI-006

3.3.4 GAIA-RVOI-008

Figure 3.12 shows the RV fit and the CCF of this candidate which points heavily towards it being a planetary candidate of mass 4.54 M_J. However, as seen in Figure 3.12(c) there is a clear bisector

correlation which solidifies RVOI-008 as a Spectroscopic Binary. We had enough datapoints for this target for the DACE in-built periodogram to provide a value for the period of the system to be 0.73 days, which did not line up with GAIA's predicted period of 0.65 days which seems to be a ratio of 19/17. In order to test if GAIA actually measured an alias of the period, we created an RV signal that GAIA would've measured for this target using the parameters that gave the best-fit RV curve (period = 0.73 days) and then made timestamps on all the dates GAIA made observations of this target throughout the years and plotted a periodogram. Obviously since the RV signal was based on a period of 0.73 days, the highest peak in the periodogram was at that value. But, Figure 3.12(d) shows a section of the periodogram which clearly has a significant peak at 0.65 days, proving that GAIA indeed measures aliases of most if not all of its exoplanet candidates.

3.3.5 GAIA-RVOI-009

RVOI-009's radial velocity curve is shown in Figure 3.13 which seems to have little to no variation in the RV magnitude relative to the size of the error bars from CORALIE. This is a strong indicator of this target being a false positive detected by GAIA.

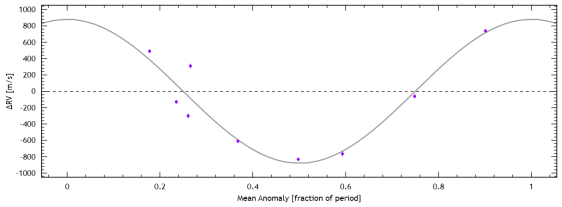

(a) RV fit of CORALIE datapoints of GAIA-RVOI-008

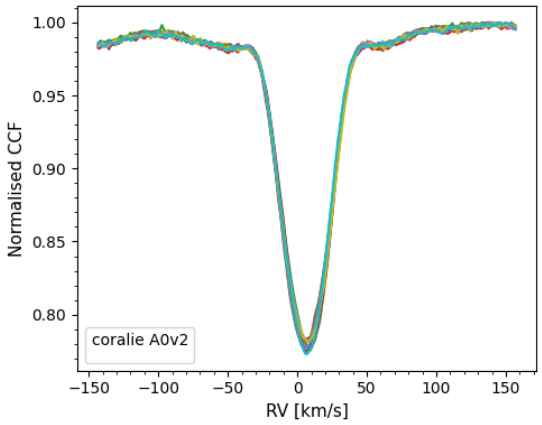

(b) GAIA-RVOI-008 CCF

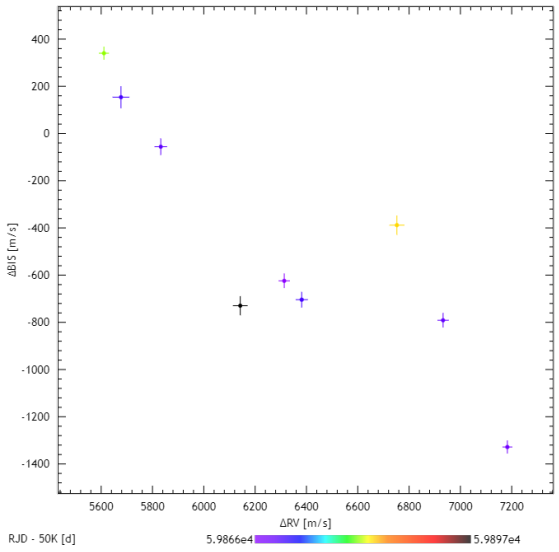

(c) RV Bisector correlation of RVOI-008

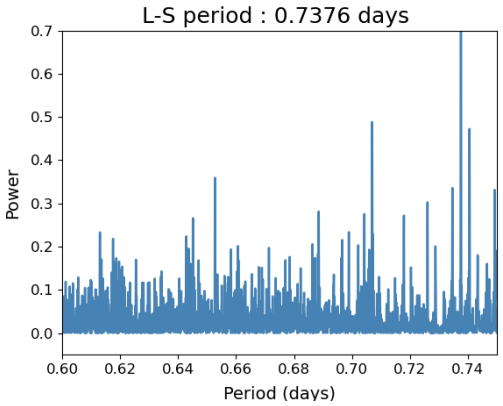

(d) Periodogram with secondary high peak at 0.65 days

Figure 3.12: Graphs highlighting the major results of RVOI-008

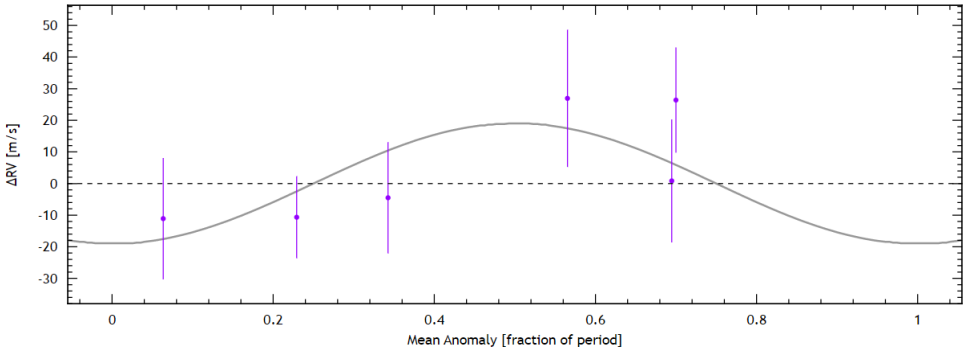

Figure 3.13: RV fit of CORALIE datapoints of GAIA-RVOI-009

Chapter 4

Conclusions

In the end, we selected 20 total exoplanet candidates from GAIA DR-3 and did some TESS lightcurve analysis and CORALIE RV follow-up to reach a conclusion about some parameters of said candidates. These candidates were selected based on the limitations of the available telescope and their visibility. Of our 20 candidates, 15 were TROIs and 5 were RVOIs and 11 of those TROIs had low cadence TESS lightcurves which allowed us to get estimates of the ephermeris and radii of the planetary candidates and compare this data to the values listed on the GAIA archive.

The main results of the lightcurve analysis were that GAIA overestimates the measured transit depth and because of its poor sampling, calculates an 'alias' of the period reported by TESS. Additionally, RV follow-ups were done for 7 of the 20 candidates so far for a total observation time equalling 3 nights, but, the actual observations were done over the course of several months (October - December). 2 of these candidates can be confirmed to be Spectroscopic Binaries, 1 is a false positive and 1 is a promising exoplanet candidate. Going forward, we plan on continuing our observations to get accurate RV follow-up on all 20 of our selected targets and reach a conclusion about their nature.

Bibliography

[1] Michel Mayor and Didier Queloz. "A Jupiter-mass companion to a solar-type star". In: 378.6555 (Nov. 1995), pp. 355–359. DOI: 10.1038/378355a0.

[2] F. Bonnarel et al. "The ALADIN interactive sky atlas. A reference tool for identification of astronomical sources". In: 143 (Apr. 2000), pp. 33–40. DOI: 10.1051/aas:2000331.

[3] ESO. *CORALIE*. 2000. URL: https://www.eso.org/public/teles-instr/lasilla/swiss/coralie/.

[4] D. Queloz et al. "From CORALIE to HARPS. The way towards 1 m s^{-1} precision Doppler measurements". In: *The Messenger* 105 (Sept. 2001), pp. 1–7.

[5] Isaac Newton Group of Telescopes. *Object Visibility - STARALT*. 2002. URL: http://catserver.ing.iac.es/staralt/.

[6] Michael Perryman. *The Exoplanet Handbook*. Cambridge University Press, 2011.

[7] Laura Kreidberg. "batman: BAsic Transit Model cAlculatioN in Python". In: *Publications of the Astronomical Society of the Pacific* 127.957 (Nov. 2015), pp. 1161–1165. DOI: 10.1086/683602. URL: https://doi.org/10.1086%2F683602.

[8] Gaia Collaboration et al. "Gaia Data Release 1". In: *Astronomy &amp Astrophysics* 595 (Nov. 2016), A2. DOI: 10.1051/0004-6361/201629512. URL: https://doi.org/10.1051%2F0004-6361%2F201629512.

[9] Gaia Collaboration et al. "The Gaia mission". In: *Astronomy &amp Astrophysics* 595 (Nov. 2016), A1. DOI: 10.1051/0004-6361/201629272. URL: https://doi.org/10.1051%2F0004-6361%2F201629272.

[10] Gaia Collaboration et al. "Gaia Data Release 2". In: *Astronomy &amp Astrophysics* 616 (Aug. 2018), A1. DOI: 10.1051/0004-6361/201833051. URL: https://doi.org/10.1051%2F0004-6361%2F201833051.

[11] Lightkurve Collaboration et al. *Lightkurve: Kepler and TESS time series analysis in Python*. Astrophysics Source Code Library. Dec. 2018. ascl: 1812.013.

[12] Ruiz-Dern, L. et al. "Empirical photometric calibration of the Gaia red clump: Colours, effective temperature, and absolute magnitude". In: *A&A* 609 (2018), A116. DOI: 10.1051/0004-6361/201731572. URL: https://doi.org/10.1051/0004-6361/201731572.

[13] Nicolas Buchschacher and Fabien Alesina. "DACE: New Available Visualisation and Analysis Tools for Exoplanet Research". In: *Astronomical Data Analysis Software and Systems XXVI*. Ed. by Marco Molinaro, Keith Shortridge, and Fabio Pasian. Vol. 521. Astronomical Society of the Pacific Conference Series. Oct. 2019, p. 757.

[14] A. Aller et al. "Planetary nebulae seen with TESS: Discovery of new binary central star candidates from Cycle 1". In: 635, A128 (Mar. 2020), A128. DOI: 10.1051/0004-6361/201937118. arXiv: 1911.09991 [astro-ph.SR].

[15] Barbara Ryden and Bradley M. Peterson. *Foundations of Astrophysics*. Cambridge University Press, 2020. DOI: 10.1017/9781108933001.

[16] Gaia Collaboration et al. "Gaia Early Data Release 3. Summary of the contents and survey properties". In: 649, A1 (May 2021), A1. DOI: 10.1051/0004-6361/202039657. arXiv: 2012.01533 [astro-ph.GA].

[17] ESA and DPAC. *Gaia Data Release 3: Documentation release 1.1*. 2022. URL: https://gea.esac.esa.int/archive/documentation/GDR3/index.html.

[18] Gaia Collaboration et al. *Gaia Data Release 3: Summary of the content and survey properties*. 2022. DOI: 10.48550/ARXIV.2208.00211. URL: https://arxiv.org/abs/2208.00211.

[19] Exoplanet Team. *The Extrasolar Planets Encyclopedia*. 2022. URL: http://exoplanet.eu/.

[20] ESA. *Transit Photometry*. n.d. URL: https://scitechdaily.com/astronomy-astrophysics-how-to-find-an-exoplanet/.

[21] NASA. *Radial Velocity Method*. n.d. URL: https://muhammadrazaa.medium.com/radial-velocity-method-detecting-exoplanets-bf3c02801d88.

[22] NASA. *TESS Observing Technical Details*. n.d. URL: https://heasarc.gsfc.nasa.gov/docs/tess/observing-technical.html.

Appendix A

Graphs

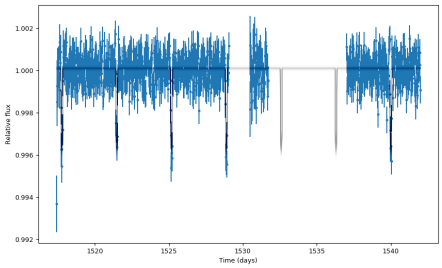

(a) GAIA-TROI-005

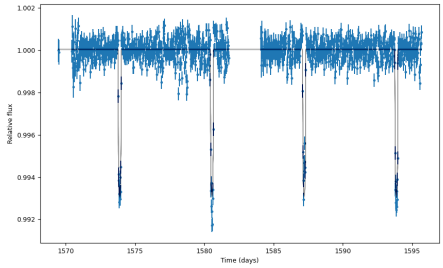

(b) GAIA-TROI-012

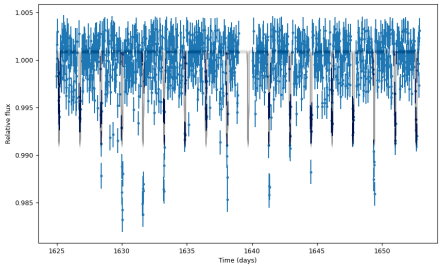

(c) GAIA-TROI-014

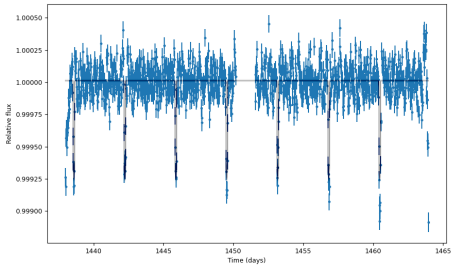

(d) GAIA-TROI-017

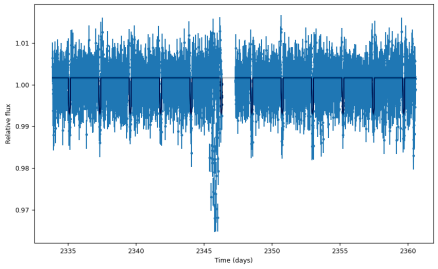

(e) GAIA-TROI-021

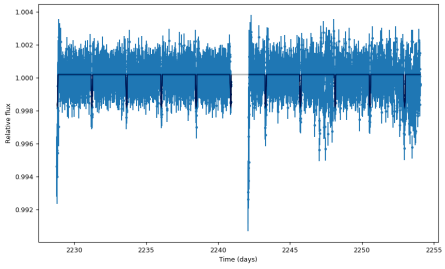

(f) GAIA-TROI-025

Figure A.1: Additional lightcurves of the TROIs

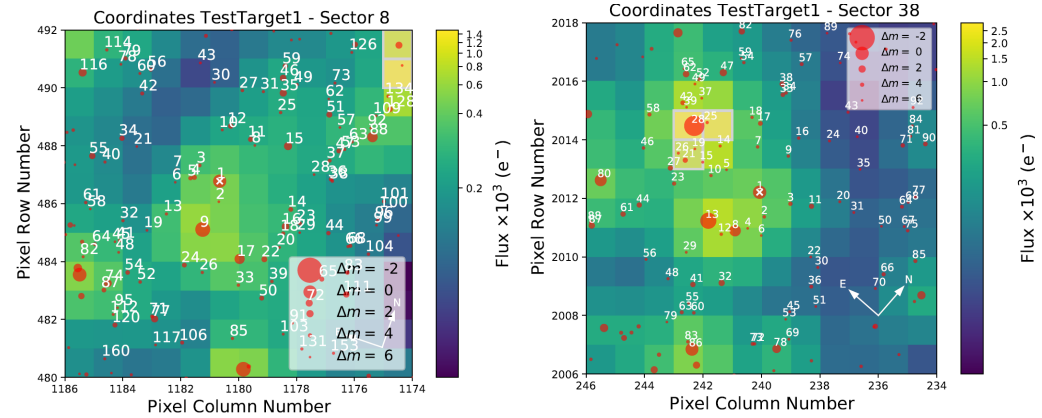

(a) GAIA-TROI-005

(b) GAIA-TROI-026

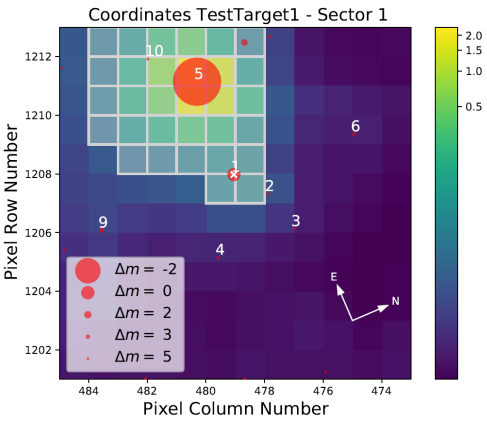

(c) GAIA-TROI-029

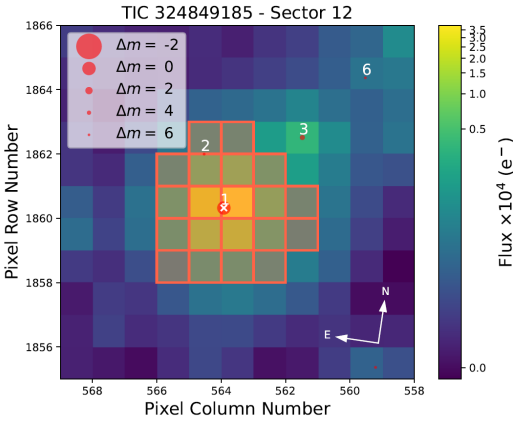

(d) GAIA-RVOI-004

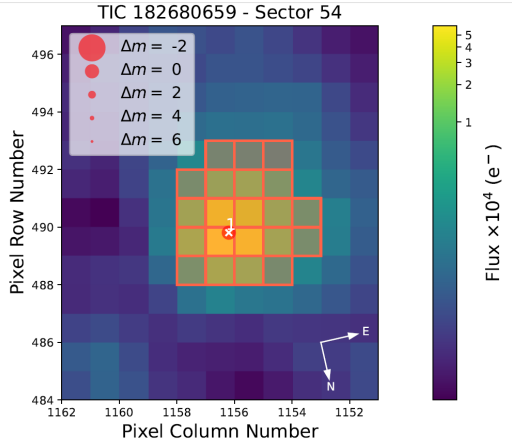

(e) GAIA-RVOI-005

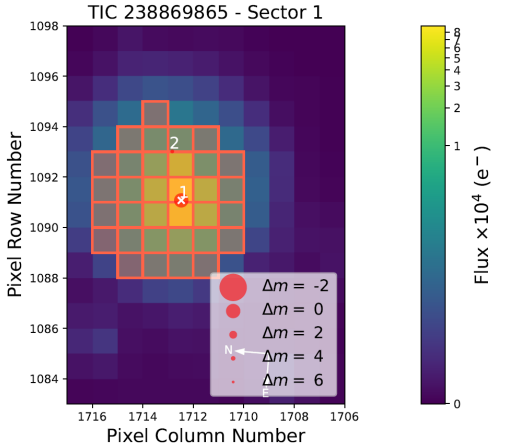

(f) GAIA-RVOI-006

Figure A.2: Additional TPFs

Appendix B

Tables

Notes B.1:
[1] TROI-020: SuperWASP (http://simbad.u-strasbg.fr/simbad/sim-ref?bibcode=2019MNRAS.488.4905S)
[2] TROI-022: Gaia DR1 (https://www.aanda.org/articles/aa/full$_h$*tml*/2018/01/*aa*31572−17/*aa*31572−17.*html*)

Table B.1: All DR3 TROIs (39)

Name	V-mag	CORALIE visibility
Gaia-TROI-003	13.205	No
Gaia-TROI-004	14.16361515	No
Gaia-TROI-005	13.24637858	Yes
Gaia-TROI-006	11.28	No
Gaia-TROI-007	12.41815956	Yes
Gaia-TROI-008	13.1410865	No
Gaia-TROI-009	14.81434883	No
Gaia-TROI-010	12.68741646	No
Gaia-TROI-011	13.73571212	No
Gaia-TROI-012	10.81	Yes
Gaia-TROI-013	12.77042857	Yes
Gaia-TROI-014	13.05927348	Yes
Gaia-TROI-015	12.72257224	No
Gaia-TROI-016	12.87500123	Yes
Gaia-TROI-017	12.43663012	Yes
Gaia-TROI-018	12.8413802	No
Gaia-TROI-019	13.54919235	No
Gaia-TROI-020	12.948	Yes (Previously confirmed Binary)[1]
Gaia-TROI-021	13.23794945	Yes
Gaia-TROI-022	9.48	No (Previously confirmed Binary)[2]
Gaia-TROI-023	12.96403617	No
Gaia-TROI-024	12.87141923	Yes
Gaia-TROI-025	13.64196478	Yes
Gaia-TROI-026	12.66952037	Yes
Gaia-TROI-027	13.70032812	No
Gaia-TROI-028	12.8948656	Yes
Gaia-TROI-029	12.57878531	Yes
Gaia-TROI-030	13.04855508	No
Gaia-TROI-031	12.69049721	Yes
Gaia-TROI-032	13.72448878	No
Gaia-TROI-033	14.19481577	No
Gaia-TROI-034	13.72635481	No
Gaia-TROI-035	14.56152273	No
Gaia-TROI-036	13.08018209	No
Gaia-TROI-037	13.48803514	No
Gaia-TROI-038	12.45859762	No
Gaia-TROI-039	11.98924509	Yes
Gaia-TROI-040	13.13468137	No
Gaia-TROI-041	13.53040563	No

Table B.2: All DR3 RVOIs (9)

Name	V-mag	CORALIE visibility	CORALIE datapoints
Gaia-RVOI-003	9.665962413	No	
Gaia-RVOI-004	8.132011591	Yes	0
Gaia-RVOI-005	7.139796177	Yes	3
Gaia-RVOI-006	6.849535619	Yes	9
Gaia-RVOI-007	7.747967963	No	
Gaia-RVOI-008	7.80756777	Yes	9
Gaia-RVOI-009	8.748461381	Yes	4
Gaia-RVOI-010	7.698056161	No	

Table B.3: Final 15 TROIs selected for analysis

Name	Period (GAIA)	RA	DEC	R_star	V-mag	Teff (GAIA)
	days	deg	deg	Stellar Radius	mag	K
TROI-005	2.56640575	137.3908125	-37.7968806	1.151293265	13.24637858	5882.065
TROI-007	16.33186347	309.542675	-3.395275	1.226486051	12.41815956	6117.19
TROI-012	3.74630053	169.9589542	-51.8660667	1.687479	10.81	5758.422
TROI-013	1.53043265	106.45015	-35.2561583	1.694502	12.77042857	5926.0024
TROI-014	1.6157177	238.9862542	-56.0904	1.539608	13.05927348	5793.2563
TROI-016	2.2086269	141.2786	-36.5795361	1.461266945	12.87500123	6910.5156
TROI-017	1.21614555	64.8730917	-25.9597917	1.404850799	12.43663012	6116.575
TROI-021	2.23583598	199.1545917	-59.0305028	1.315284135	13.23794945	6525.583
TROI-024	1.81669543	259.1638542	-14.9108	1.062960653	12.87141923	5867.7256
TROI-025	1.61149966	109.9301625	-20.090425	1.465117165	13.64196478	6233.344
TROI-026	2.02375893	194.1472583	-51.961625	1.519103751	12.66952037	6521.042
TROI-028	0.99927053	118.736975	-32.3560944	1.065469726	12.8948656	6003.0547
TROI-029	4.58295142	67.933	-61.3859361	1.112158012	12.57878531	5821.2383
TROI-031	2.83165794	175.6271458	-52.6274278	1.30393583	12.69049721	6075.2593
TROI-039	1.9465478	319.1818583	-1.9432778	1.321642446	11.98924509	6037.8306

Table B.4: Comparing GAIA and TESS periods

Name	TPF	TESS lightcurve	Period (GAIA)	Period (TESS)	P_TESS/P_GAIA	CORALIE
			days	days		Datapoints
TROI-005	Yes	Yes	2.56640575	3.726465	13/9 or 16/11	0
TROI-007	No	No	16.33186347			1
TROI-012	Yes	Yes	3.74630053	6.662605	16/9	0
TROI-013	No	Yes	1.53043265	1.531435	1.0006	7
TROI-014	No	Yes	1.6157177	1.616244	1.0003	0
TROI-016	No	No	2.2086269	2.2120254		0
TROI-017	Yes	Yes	1.21614555	3.640805	2.9937	5
TROI-021	No	Yes	2.23583598	2.23583598	1	0
TROI-024	No	No	1.81669543			0
TROI-025	No	Yes	1.61149966	2.4142	1.498	0
TROI-026	Yes	Yes	2.02375893			0
TROI-028	No	Yes	0.99927053			0
TROI-029	Yes	Yes	4.58295142			0
TROI-031	No	Yes	2.83165794			0
TROI-039	No	No	1.9465478			0

Table B.5: Final 5 RVOIs selected for analysis

Name	**Period (GAIA)**	**RA**	**DEC**	**M_star**	**V-mag**	**Teff (GAIA)**
	days	hh:mm:ss	hh:mm:ss	Stellar Mass	mag	K
RVOI-004	3.519025934	16 34 48.638	-65 52 34.32	1.25	8.132011591	6277.676
RVOI-005	4.520330813	19 18 23.309	05 07 51.75	1.28	7.139796177	6323.499
RVOI-006	0.6483842676	02 33 16.541	-75 53 36.60	1.39	6.849535619	6485.0737
RVOI-008	0.6592772471	21 07 55.973	-22 20 7.16	1.632	7.80756777	7152.908
RVOI-009	1.217681717	00 08 10.287	25 18 1.15	1.391	8.748461381	6626.7124

Table B.6: Comparing the RV semi amplitude (K) from GAIA and CORALIE

Name	Period (GAIA)	K (GAIA)	K (CORALIE)	K consistency?
	days	km/s	km/s	
RVOI-004	3.519025934	0.811		N/A
RVOI-005	4.520330813	1.322	3.544	No
RVOI-006	0.6483842676	1.58	0.046	No
RVOI-008	0.6592772471	2.084	0.879	No
RVOI-009	1.217681717	1.946	0.019	No